Received: 14 February 2019 | Revised: 11 November 2019 | Accepted: 13 January 2020

DOI: 10.1002/jemt.23451

RESEARCH ARTICLE

MICROSCOPY RESEARCH & TECHNIQUE WILEY

# OM, SEM–EDX, and micro-FTIR analysis of the Bronze Age pottery from the Băile Figa salt production site (Transylvania, Romania)

Viorica Vasilache[1] | Valerii Kavruk[1,2] | Felix-Adrian Tencariu[1]

[1]Interdisciplinary Research Department—Field Science, Arheoinvest Platform of Interdisciplinary Research in Archaeology, Alexandru Ioan Cuza University of Iaşi, Iaşi, Romania

[2]The National Museum of Eastern Carpathians, Sfântu Gheorghe, Romania

**Correspondence**
Viorica Vasilache, Interdisciplinary Research Department—Field Science, Arheoinvest Platform of Interdisciplinary Research in Archaeology, Alexandru Ioan Cuza University of Iaşi, Lascar Catargi St., 54, 700107 Iaşi, Romania.
Email: viorica_18v@yahoo.com

**Funding information**
CNCS - UEFISCDI, Grant/Award Number: PN-III-P4-ID-PCE-2016-0759

**Review Editor:** Paul Verkade

## Abstract

This article presents the results of analyses carried out on a lot of 11 fragments of Bronze Age ceramics discovered in the site from Băile Figa (Beclean town, Transylvania, Romania), where salt exploitation occurred. The samples were analyzed by means of optical microscopy, on the basis of which the morphology and distribution of the inclusions in the ceramic paste was established. Likewise, the samples were analyzed by scanning electron microscopy with energy-dispersive X-ray spectrometry, producing microphotographs for each sample, and on the basis of the X-ray spectra, the elemental composition in gravimetric percentages was established. Through the micro-Fourier-transform infrared spectroscopy analysis, on the basis of characteristic group vibrations, it was possible to ascertain the nature of the compounds from the ceramic samples. These analyses will contribute to the reconstruction of the prehistoric technologies for salt exploitation.

**KEYWORDS**

Bronze Age, ceramics, micro-FTIR, OM, SEM–EDX

## 1 | INTRODUCTION

Ceramics, both as a material with multiple uses and as a manufacturing technology, is a complex combination of previous areas of knowledge and human experience, resources, management (clay, additives, fuels), technological processes/operations, innovation, and needs (storage and preservation of products, food preparation in suitable containers, aesthetic needs etc.; Rice, 1999).

The properties of ancient ceramics differ, even when using the same clay, depending on the complexity of the objects made, the firing temperatures, the duration and the amount of oxygen present during firing, manner/degree of use, and the lying conditions in the archaeological site (Drebushchak, Mylnikova, Drebushchak, & Boldyrev, 2005; Iordanidis, Garcia, Guinea, & Karamitrou Mentessidi, 2009; Sandu et al., 2010; Sandu, Vasilache, Tencariu, & Cotiugă, 2010).

With regard to the importance of studying ancient ceramics, any fragment found is valuable, providing, through its components, the manufacturing technology and presumable functions, valuable information about its life cycle, and, more important, about the society which created it (Sandu, Cotiugă, et al., 2010; Sandu, Vasilache, et al., 2010; Tite, 1999).

The use of modern investigative techniques of ceramic fragments found in archaeological sites allows establishing the chemical nature of the constructive components, the microstructure and layout of the mineralogical elements, the temperature and type of firing, the usage, the object's use-life and archaeological setting (by setting the context), conservation status, and other archaeometric and ceramological characteristics (Cotiugă et al., 2012; Sandu, Cotiugă, et al., 2010; Sandu, Vasilache, et al., 2010).

The investigation of ancient ceramics usually employs nondestructive or paradestructive, noninvasive methods that allow direct operations on the object, such as visual analysis using measuring tools, reflectography, profilometry, and colorimetry by reflection, radiography, etc. These procedures often require information concerning the object's chemical, mineralogical, and crystallographic properties, which in turn can be obtained via analyses of the internal structure: at the breaking points

  

in the stratigraphic section or of the powder (Benedetto, Laviano, Sabbatini, & Zambonin, 2002; Hajjaji, Kacim, & Boulmane, 2002; Ionescu, Ghergari, Horga, & Radulescu, 2007; Maggetii, 1994). The newest methods of sampling and processing involve interdisciplinary techniques employing co-assistance or conjunction systems, such as scanning electron microscopy with energy dispersive X-ray spectrometry (SEM–EDX; Froh, 2004; Goodall, Hall, Viel, & Fredericks, 2007; Merkevicius et al., 2007; Velraj, Tamilarasu, & Ramya, 2015); micro-Fourier-transform infrared spectroscopy (micro-FTIR; Barilaro et al., 2008; Gaboyer et al., 2017; Manoharan, Venkatachalapathy, Dhanapandian, & Deenadayalan, 2007; Naseerutheen, Ravisankar, Rajalakshmi, Raja Annamalai, & Chandrasekaran, 2013; Palanivel & Velraj, 2007; Shoval, 2003); micro-Raman (Goodall et al., 2007) and thermal analysis (Krapukaityte, Tautkus, Kareiva, & Zelickiene, 2008; Palanivel & Rajesh Kumar, 2011; Velraj, Janaki, Mohamed Musthafa, & Palnivel, 2009); Inductively Coupled Plasma - ICP, Neutron Activation Analysis - NAA, and portable X-ray Fluorescence - pXRF (Forster, Grave, Vickery, & Kealhofer, 2011; Hunt & Speakman, 2015; Mitchell, Grave, Maccheroni, & Gelman, 2012; Tsolakidou, Buxeda, Garrigós, & Kilikoglou, 2002; Tsolakidou & Kilikoglou, 2002); and others (Papachristodoulou, Oikonomou, Ioannides, & Gravani, 2006; Ravisankar et al., 2011; Sandu, Vasilache, et al., 2010).

This study focuses on some Bronze Age potsherds from the *Băile Figa* salt production site (Cavruc et al., 2015; Harding & Kavruk, 2013).

The site is located in northeast Transylvania, on the administrative territory of Beclean town, Bistriţa Năsăud County, Romania (Figure 1). It superposes the rock salt deposit and is rich in brine, salt mud, and halophytes. The research studies carried out in 2005–2018 have uncovered extensive salt-production remains dating from between circa 3500 BC and the 20th century AD. Most of the evidence uncovered in the site dates back to the Bronze Age (ca. 2400–800 BC).

The Early Bronze Age (EBA) evidence was mainly uncovered at the northern end of the site, in salt mud, above the rock salt deposit, in the stream bed, and in the valley of the salty brook. It includes pottery that often has a brushed and/or textile imprinted surface, specific to the *Gornea-Foeni* culture (ca. 2400/2300 to 2000/1900 BC).

The Late Bronze Age (LBA) evidence was found to date from circa 1600/1500 to 900/800 BC. They were spread across the entire site

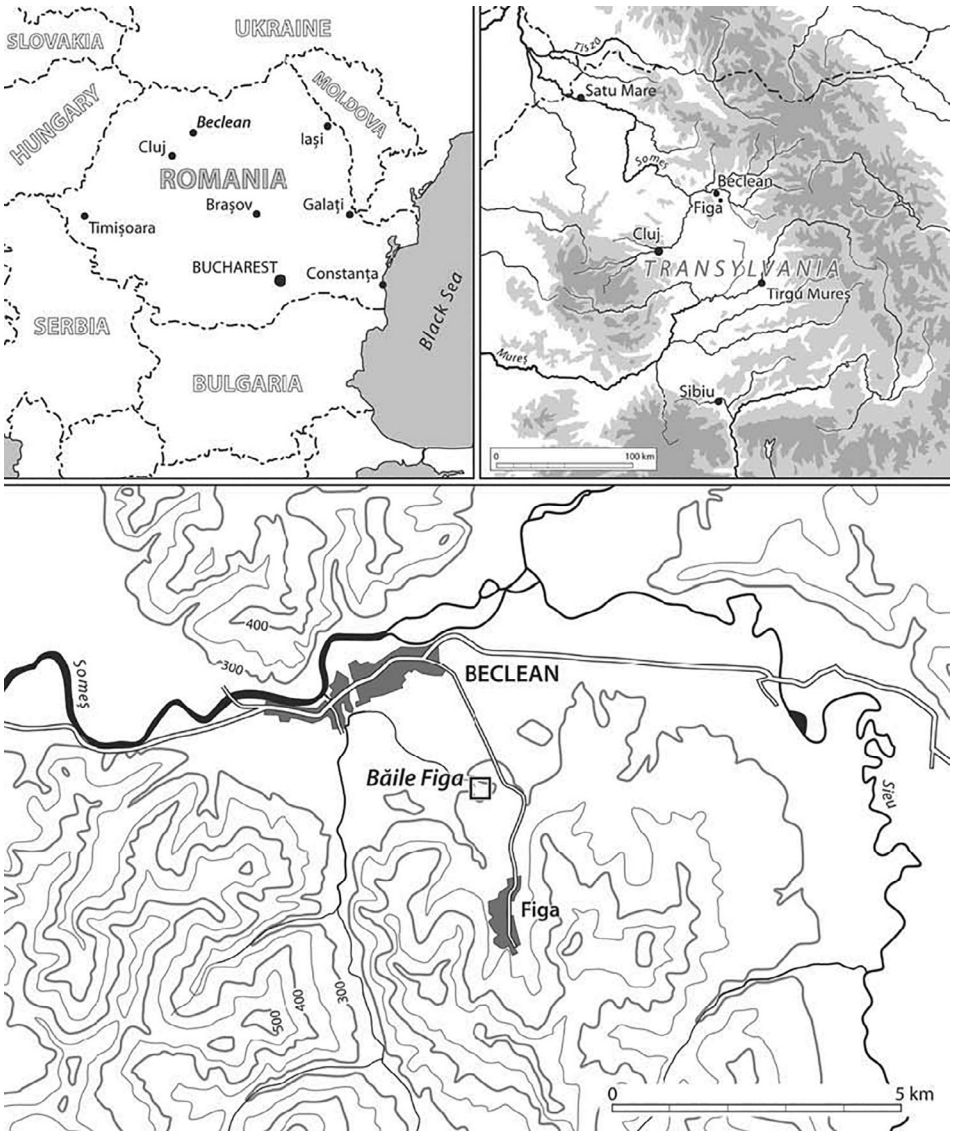


**FIGURE 1** Location map for Băile Figa (Harding & Kavruk, 2013)

and include timber structures; troughs and channeled pieces made of tree trunks; wooden shovels, hammers, and wedges; a wooden ladder; a number of stone mining hummers; and fragmented pottery. Most of the LBA pottery was found in the northern part of the site, in salt mud, above the rock salt deposit, among wooden structures, and artifacts that predominantly date from the 12th to 9th centuries BC. Most of this pottery had a brushed surface and showed close similarities to the pottery specific to the *Lăpuş* culture (ca. 1400–1100- BC). This pottery seems to date little earlier than the timber structures mentioned above.

Work at Băile Figa recovered 4,095 sherds weighing 56.172 kg in different parts of the site. Pottery was found only in Trenches I, III, V, VI, and VII. Of the total quantity of the pottery recovered, 3,622 sherds (50.076 kg) can be attributed to prehistoric periods (mainly Bronze and Iron Ages) and 473 sherds (6.096 kg) to the postmedieval or modern periods (19th–20th centuries AD). The distribution of the pottery recovered on the site is quite uneven, which is given as follows: Trench I: 359 sherds (5.605 kg), of which 17 (0.606 kg) were Bronze Age, 40 (1.096 kg) Iron Age, and 302 (3.903 kg) postmedieval/modern; Trench III: 3,116 sherds (42.969 kg), of which 1 was possible Neolithic, 2,946 (40.810 kg) Bronze Age (predominantly EBA), and 170 (2.159 kg) postmedieval/modern; Trenches V and VI: 60 sherds, of which 50 were Bronze Age (mostly LBA) and 10 postmedieval or modern; Trench VII: 611 sherds (7.444 kg), of which 513 Bronze Age (mostly LBA) and 98 undatable (small and undistinctive).

Taking into account the context in which the EBA and LBA pottery has been found, it would be reasonable to assume that it has been used in salt production, most probably in brine processing. In order to verify this assumption, we need to answer at least the following questions: Whether the BA pottery found in the northern part of the site bears any chemical and physical traits of salt processing? What from and how this pottery has been manufactured? Whether and to what extent the pottery fabric and manufacturing was aimed to produce the wares suitable for salt production?

At the same time, it is important to reveal as many as possible details concerning the pottery fabric content and of the pottery manufacturing, in order to be able to produce replicas according to the results of analytical investigations. The replicas will be used in ethno-archaeological experiments, which will suggest whether and how this pottery was used in salt production.

The present study aims to determine the chemical nature of the fabric components, the microstructure and the combination of the mineralogical elements, the temperature and type of burning, as well as the mode of use and postdepositional change of 11 Bronze Age sherds. The first steps to achieve these goals are optical microscopy (OM), SEM–EDX, and micro-FTIR.

## 2 | MATERIALS AND METHODS

Analyses were performed on 11 potsherds. Each was assigned an ID code that started with the alphabet "S" followed by the inventory number (Figure 2).

The earliest of the analyzed ceramic fragments (S15157) was discovered in Trench VII (Figure 3), in a secondary position, in greyish brown soil of the filling of Pit no. 3 (5 × 3 m), which was slightly deepened (up to 0.7 m) into sterile soil (yellow clay). The fragment fabric content, the shape, and the processing of its surfaces indicate that it belongs the Gornea-Foeni culture of the final stage of the EBA.

The other 10 ceramic fragments analyzed (S14763, S15150, S15278, S15282, S15317, S15321, S16642, S16645, S16667, and S17713) were discovered in Trench III (Figure 3), in a secondary position, in the mud layer, at various depths, among the traces of wooden structures dating from circa 1200 to 800 cal. BC (Harding & Kavruk, 2013). The discovery conditions and the morphological features of these potsherds argue for their slight anteriority with respect to the wooden structures from the same trench. The closest analogies for this pottery are known in the Lăpuş (14th–12th centuries BC) spread in Northern Transylvania (Kacsó, Metzner-Nebelsick, & Nebelsick, 2011).

The analyses performed on the ceramic fragments were made on the black and red areas, those corresponding to the types of reducing and oxidizing firing, in order to verify if the firing atmosphere influences the elemental composition of the samples.

The ceramic fragments were cut and polished using a Struers LaboPol grinder–polisher using disks of various granulations and subsequently analyzed by means of OM using a Zeiss Imager a1M microscope with an Axiocam camera attached. The analyses were carried out by reflection at ×50 magnification in the dark field.

One of the aims of the research is to ascertain the use of the vessels in the exploitation and production of salt, by means of physical–chemical analyses.

For highlighting the structural characteristics and the elemental composition, we employed an SEM model Vega II LSH produced by Tescan, coupled to an EDX detector model Quantax QX2 produced by Bruker/Roentec Germany, and a specialized software for processing spectral data, capable of operating in a BSE regimen (secondary electrons retrodiffused or scattered) and SE (secondary electrons). Microphotographs of the analyzed samples were obtained using a BSE detector at ×500 magnification. The analyzed fragments were not covered with carbon, since in the ceramic analysis this element is an indicator of the firing temperature and this would have contaminated the samples.

The samples that showed the presence of carbon in their composition were analyzed using an FTIR spectrophotometer coupled to a Hyperion 1000 microscope, both produced by Bruker Optic, Germany.

The FTIR spectrophotometer is a model Tensor 27, which is foremost suitable for measurements in the near IR. The standard detector is DLaTGS, which covers the spectral domain 7500–370 $cm^{-1}$, and works at room temperature. The standard resolution is 4 $cm^{-1}$, but it can also reach 1 $cm^{-1}$. Tensor 27 is fitted with an He–Ne laser, which emits at 633 nm and a power of 1 mW, presenting a Rocksolid alignment of the interferometer. The signal/noise ratio of this spectrophotometer is very good. Tensor 27 is fully controlled through the Opus software.

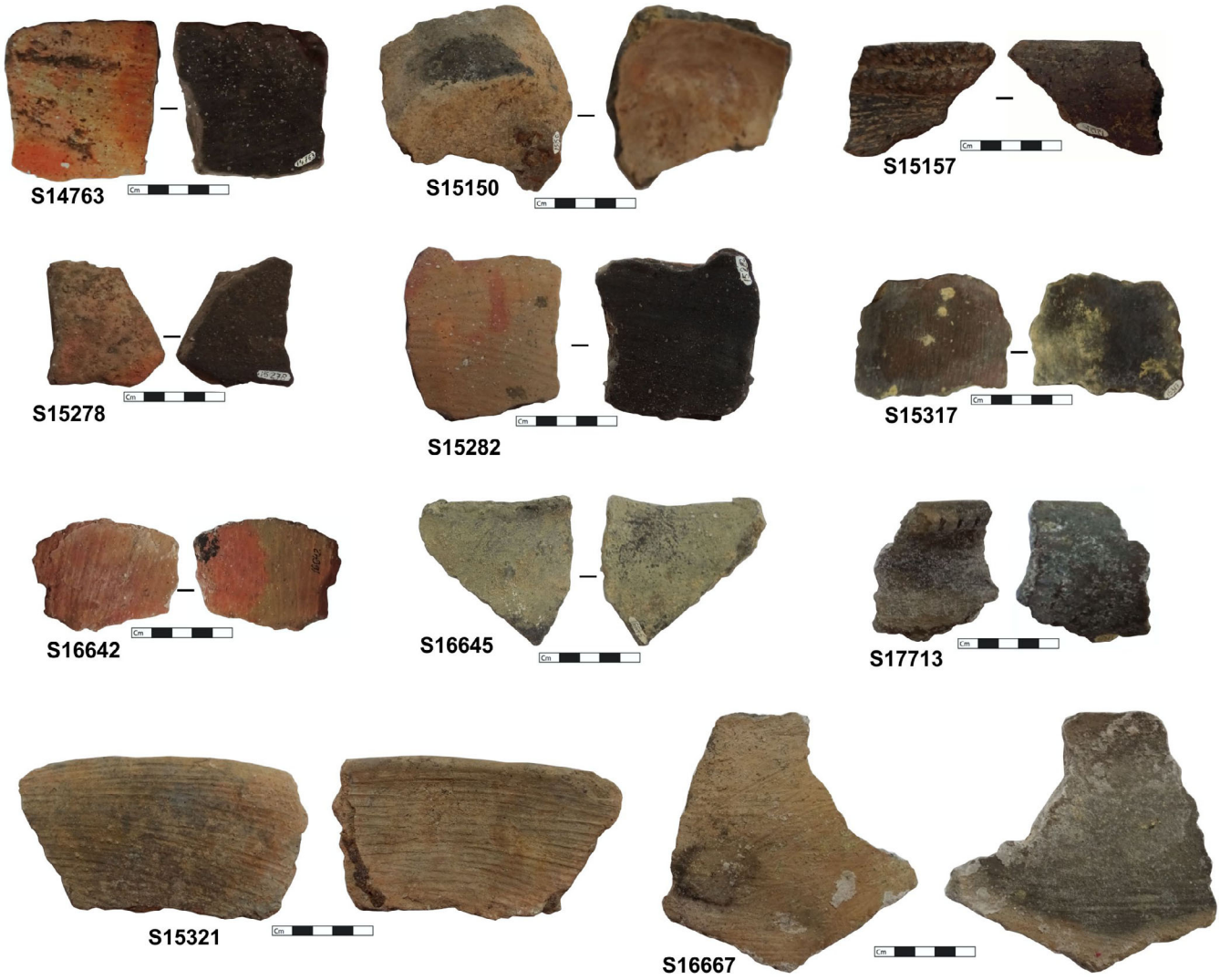


**FIGURE 2** Front and back views of the analyzed ceramic fragments [Color figure can be viewed at wileyonlinelibrary.com]

The Hyperion 1000 microscope is an accessory that can be coupled with almost any FTIR spectrophotometer produced by Bruker. For fully nondestructive readings, the Tensor 27 spectrophotometer is coupled to the Hyperion 1000 microscope; usually, for solid samples, the work is done in reflectance mode.

The software used is Opus/Video for the acquisitioning of interactive video data. It is possible to work both in transmission and reflection modes. The detector is an MCT type, cooled with liquid nitrogen (−196°C).

The spectral domain in which the work was carried out was 600–4000 $cm^{-1}$, and the measured area is optimized at a diameter of 250 μm, with the possibility to reach a minimum of 20 μm. The microscope is fitted with a ×15 lens.

The equipment used for the analyses is part of the infrastructure of the Laboratory of Scientific Investigation and Conservation of Cultural Heritage from within the Arheoinvest Platform of Archaeological Research of the "Alexandru Ioan Cuza" University of Iaşi.

## 3 | RESULTS AND DISCUSSION

The technological study of the 11 fragments comprises observations regarding the forming and decoration techniques, the burning technique, and the fabric, based on macroscopic and microscopic investigation of the clay matrix (in terms of color, inclusions, pores). Thus,

- the fragment S14763 (Figure 4) has a thickness of 14 mm, presents mainly lithoclast inclusions (0.5 mm), rounded and subangular, well-threaded paste, both surfaces decorated with striations, reducing firing, followed by oxidation;
- the fragment S15150 (Figure 5) has a thickness of 7 mm, presents an inner slip with small ceramoclasts, paste without inclusions, only with traces of plant remains, well-threaded paste, reducing firing;
- the fragment S15157 (Figure 6) has a thickness of 9 mm, mainly lithoclast inclusions, subrounded, poorly threaded paste, reducing firing;

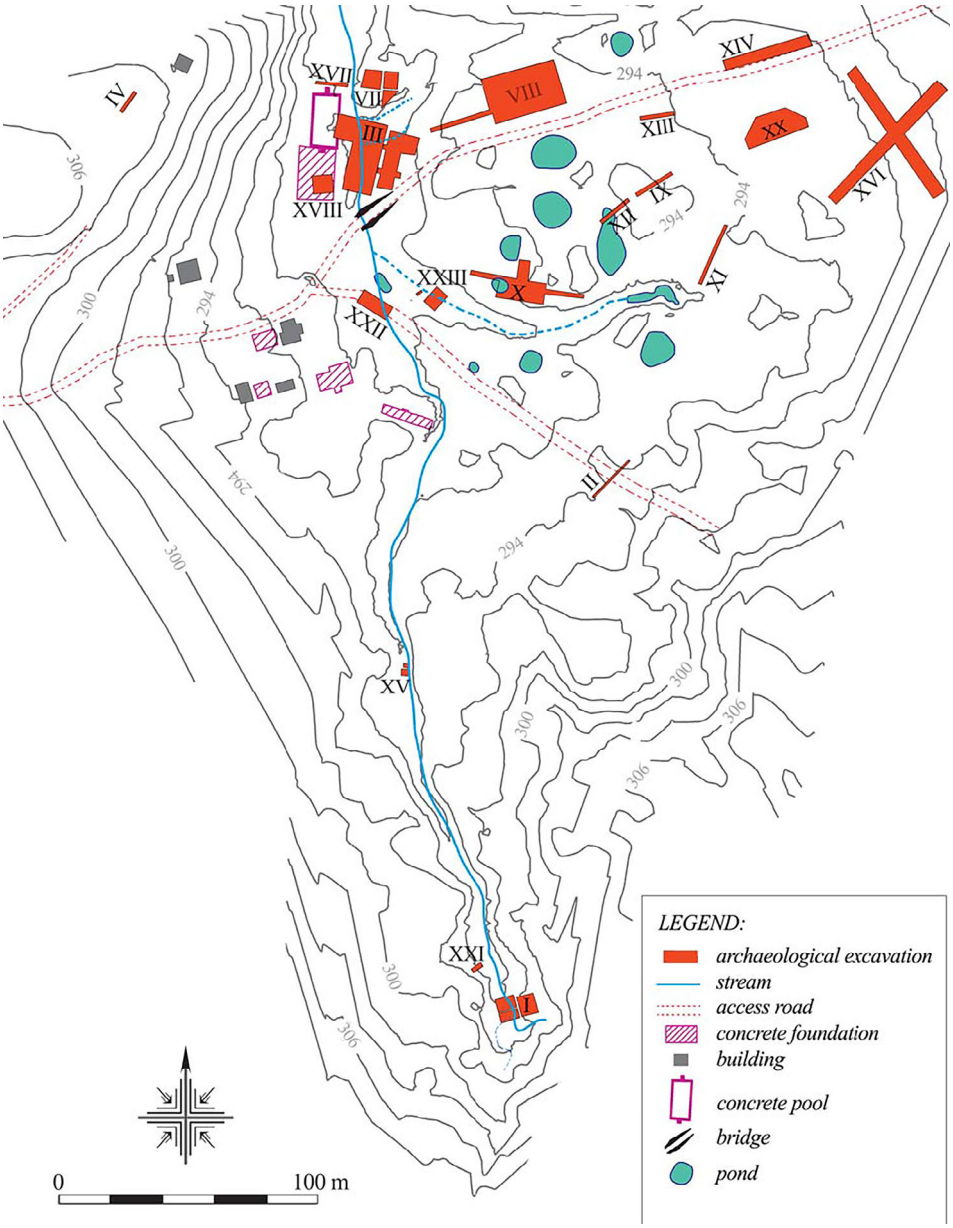


**FIGURE 3** The topographic plan of the Băile Figa site (Harding & Kavruk, 2013) [Color figure can be viewed at wileyonlinelibrary.com]

- the fragment S15278 (Figure 7) with a thickness of 13 mm has mainly small lithoclast inclusions, subrounded, well-threaded paste, incomplete reducing firing;
- the fragment S15282 (Figure 8) with a thickness of 13 mm presents mainly small lithoclast inclusions under 0.5 mm, rounded, well-threaded paste, both surfaces decorated with striations, reducing firing followed by oxidation;
- the fragment S15317 (Figure 9) has a thickness of 7 mm with mainly lithoclast inclusions, sufficiently threaded paste, outer surface decorated with striations, incomplete oxidative firing (possibly fired with the mouth on the ground);
- the fragment S15321 (Figure 10) with a thickness of 14 mm has mainly lithoclast inclusions, subrounded and subangular, well-threaded paste, both surfaces decorated with striations, oxidative firing;
- the fragment S16642 (Figure 11) with a thickness 12 mm has mainly lithoclast inclusions, subangular and angular, sufficiently threaded paste, both surfaces decorated with striations, incomplete reducing firing;
- the fragment S16645 (Figure 12) with a thickness of 8 mm has mainly lithoclast inclusions of large size (1.5–2 mm), subangular and angular, well-threaded paste, reducing firing;
- the fragment S16667 (Figure 13) with a thickness of 13 mm has mainly lithoclast inclusions, rounded and subangular, poorly threaded paste, both surfaces decorated with striations and external slip, incomplete reducing firing followed by oxidation;
- the fragment S17713 (Figure 14) has a thickness of 11 mm with mainly lithoclast inclusions, ceramoclasts of various sizes, angular lithoclasts, subrounded 0.5–2 mm ceramoclasts, poorly threaded paste, inner surface decorated with striations, external slip, reducing firing;

The colors were defined using the Munsell Soil Color Charts (Munsell Color, 2009). Macroscopic and microscopic observations

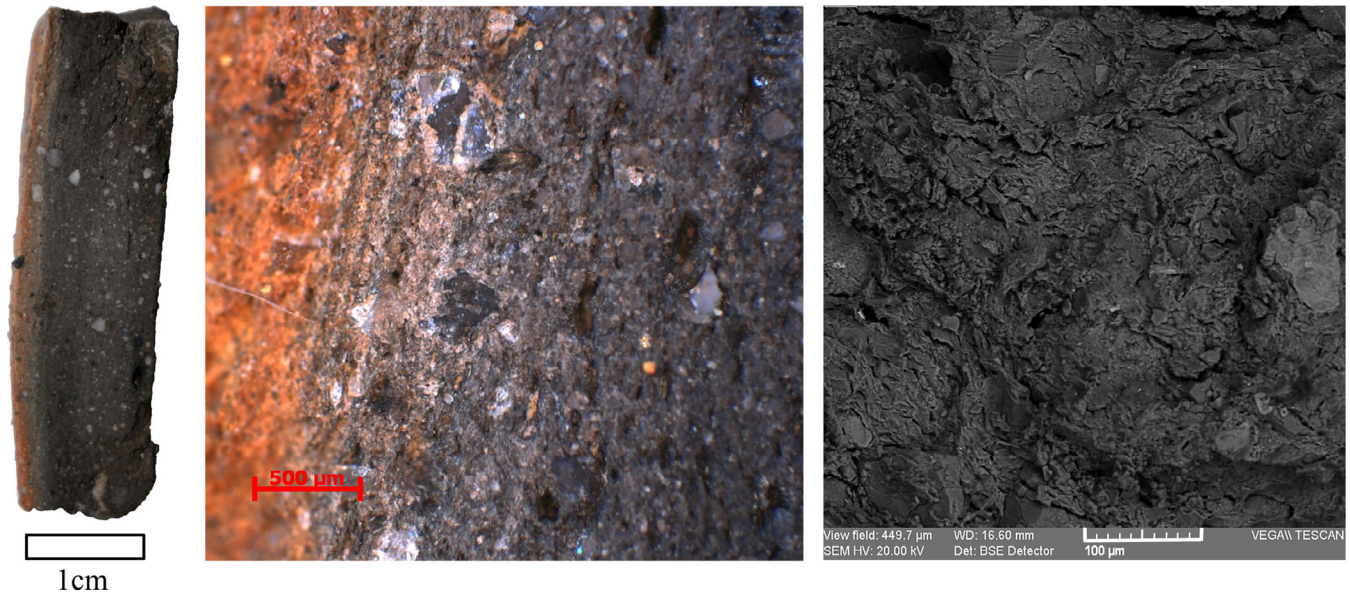


**FIGURE 4** Sample S14763: (a) macroscopic photograph, (b) OM and (c) SEM images. OM, optical microscopy; SEM, scanning electron microscopy with energy-dispersive X-ray spectrometry [Color figure can be viewed at wileyonlinelibrary.com]

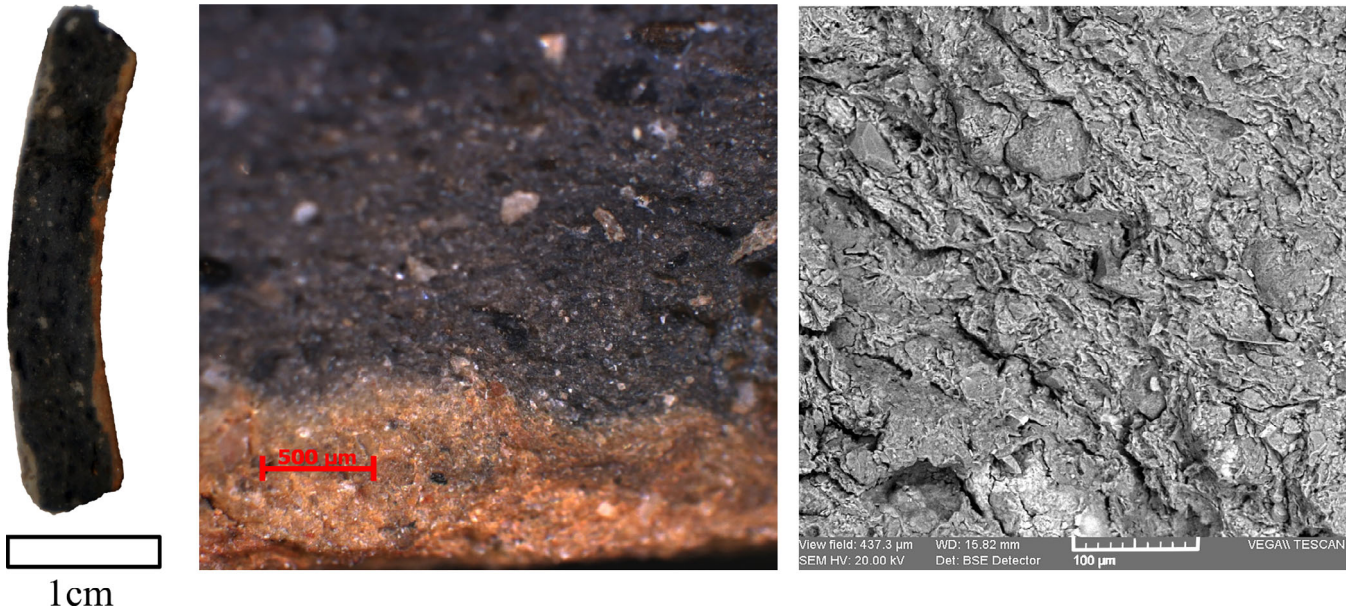


**FIGURE 5** Sample S15150: (a) macroscopic photograph, (b) OM and (c) SEM images. OM, optical microscopy; SEM, scanning electron microscopy with energy-dispersive X-ray spectrometry [Color figure can be viewed at wileyonlinelibrary.com]

were made on fresh breaks and grounded edges. With regard to the manufacturing technique, all the fragments originate from hand-thrown pots most likely fashioned from clay coils (some of the fragments display vague traces of the coils' merges). With respect to the finishing of the surfaces and the decoration, most (eight) of the fragments have both surfaces smoothed roughly, and seven samples have surfaces with striations and/or broom decorations (Besenschtrich Keramik—Figure 2). Three sherds (the thinnest of the lot—S15150, S16645, and S15317) have more carefully smoothed inside surfaces. Besides the striations, only two fragments have decoration: S15157 has an alveolated rope decoration under the mouth, while S17713 has slightly oblique notches on the lip (Figure 2).

On what concerns the fabric, except for one sample (S15150) that has a fine-grained matrix, with inclusions less than 5%, all the other samples belong to coarse or semi-coarse pottery (7–30% inclusions, with bad to moderate sorting). The main inclusions consist of milky quartz grains, angular and subangular, with sizes varying from 100 µm to 1–1.5 mm. Other inclusions, very rare, are grog and other rock fragments. The various sizes and mostly angular shapes of the inclusions could indicate that they were added

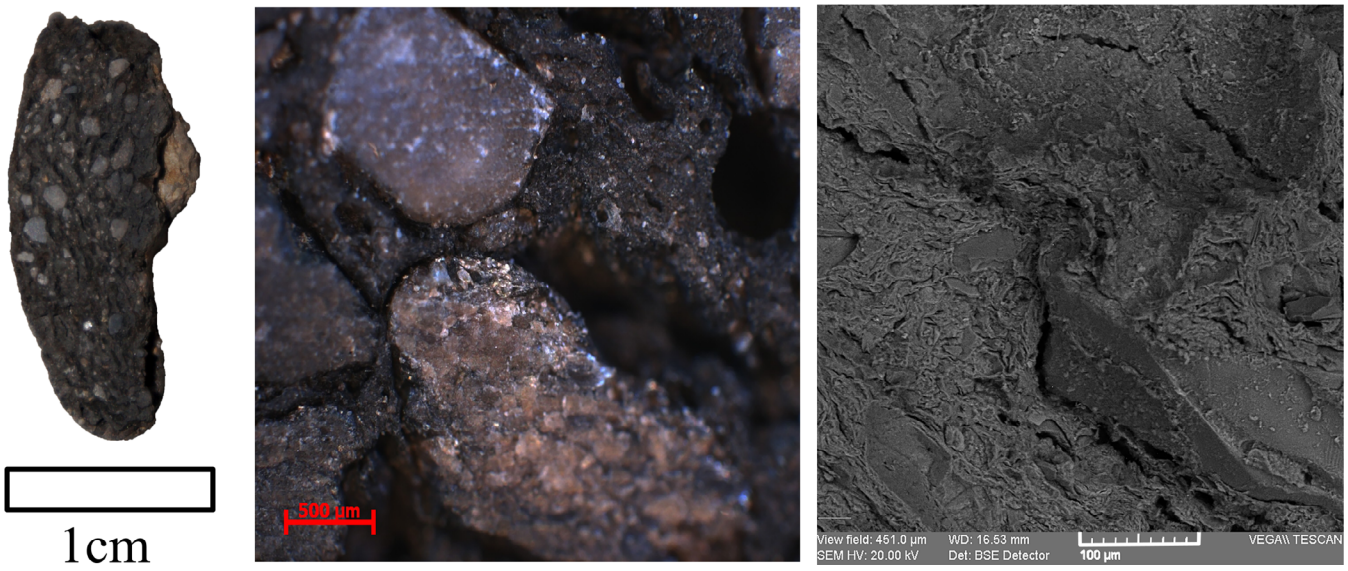


**FIGURE 6** Sample S15157: (a) macroscopic photograph, (b) OM and (c) SEM images. OM, optical microscopy; SEM, scanning electron microscopy with energy-dispersive X-ray spectrometry [Color figure can be viewed at wileyonlinelibrary.com]

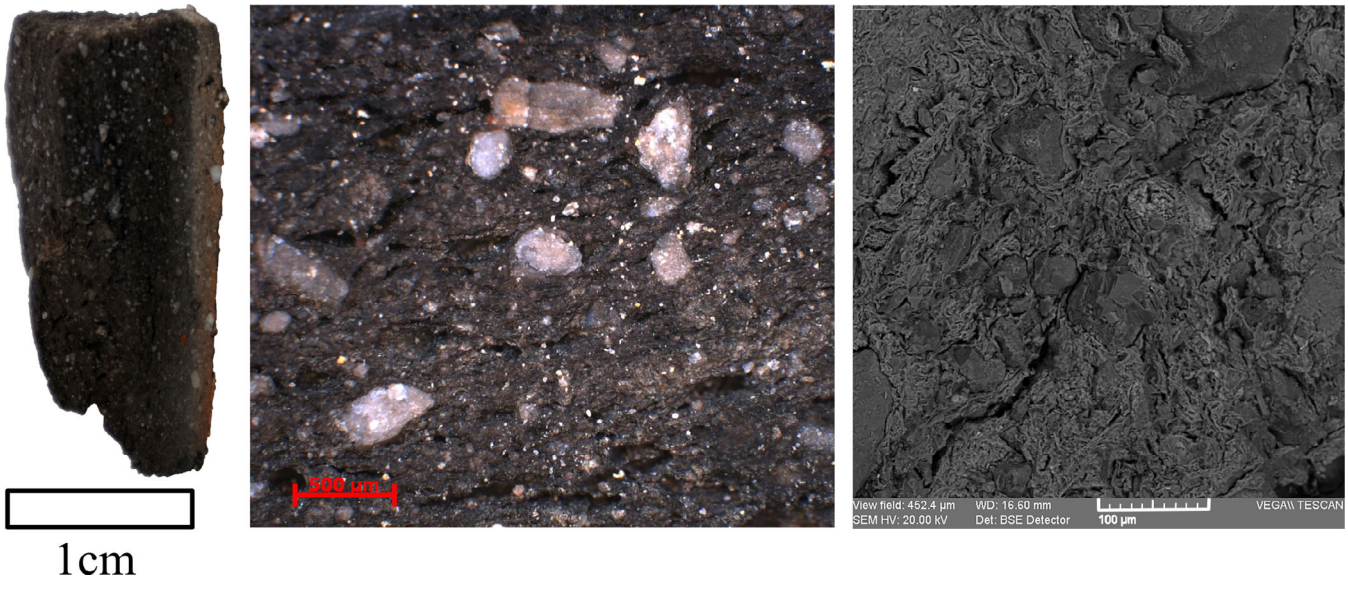


**FIGURE 7** Sample S15278: (a) macroscopic photograph, (b) OM and (c) SEM images. OM, optical microscopy; SEM, scanning electron microscopy with energy-dispersive X-ray spectrometry [Color figure can be viewed at wileyonlinelibrary.com]

deliberately to the clay by the potter, probably to enhance the thermal resistance of the vessels.

The colors of the Băile Figa samples provide some information on the firing technique and subsequent use. While most of the potsherds have a black or very dark grey (5YR3/1) core (nine samples), the surface colors (layers of 1–3 mm) are lighter, varying within the range of light brownish grey (10YR6/2), grey (5YR6/1), dark grey (5YR4/1), pale brown (10YR6/3), brown (7.5YR5/4), reddish yellow (5YR6/6), yellowish red (5YR5/6), reddish grey (5YR5/2), and red (2.5YR5/8). In one case (S15321), the color is lighter across the entire thickness (reddish brown, 5YR5/4), while in another (S15317), the color is lighter (dark reddish brown, 5YR3/4) along approximately two thirds of the section—the outside part—and very dark grey (5YR3/1) toward the interior. These characteristics suggest that the ceramics were fired rather superficially, in pits or simple kilns, in a reducing or neutral atmosphere. The lighter and uneven color of the surfaces can also be due to a weak oxidation during the use of the pots, probably in an open fire.

The EDS analysis was carried out in the section in areas of different colors, corresponding to the types of firing identified, and the results are centralized in Table 1. Thus, with the exception of sample S15157 that does not contain Cl, in all other ceramics, the following chemical elements were identified: Si, Al, Fe, Ca, Mg, K, Na, Ti, Cl, and O, which correspond to the lithic material used and the

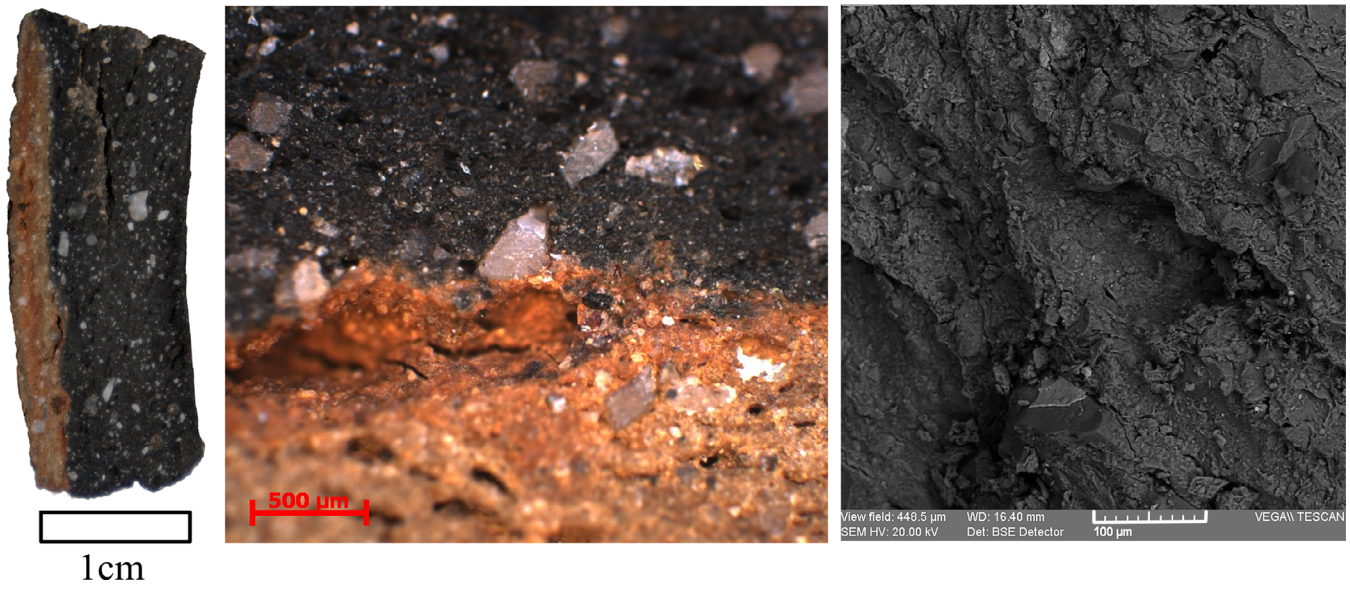


**FIGURE 8** Sample S15282: (a) macroscopic photograph, (b) OM and (c) SEM images. OM, optical microscopy; SEM, scanning electron microscopy with energy-dispersive X-ray spectrometry [Color figure can be viewed at wileyonlinelibrary.com]

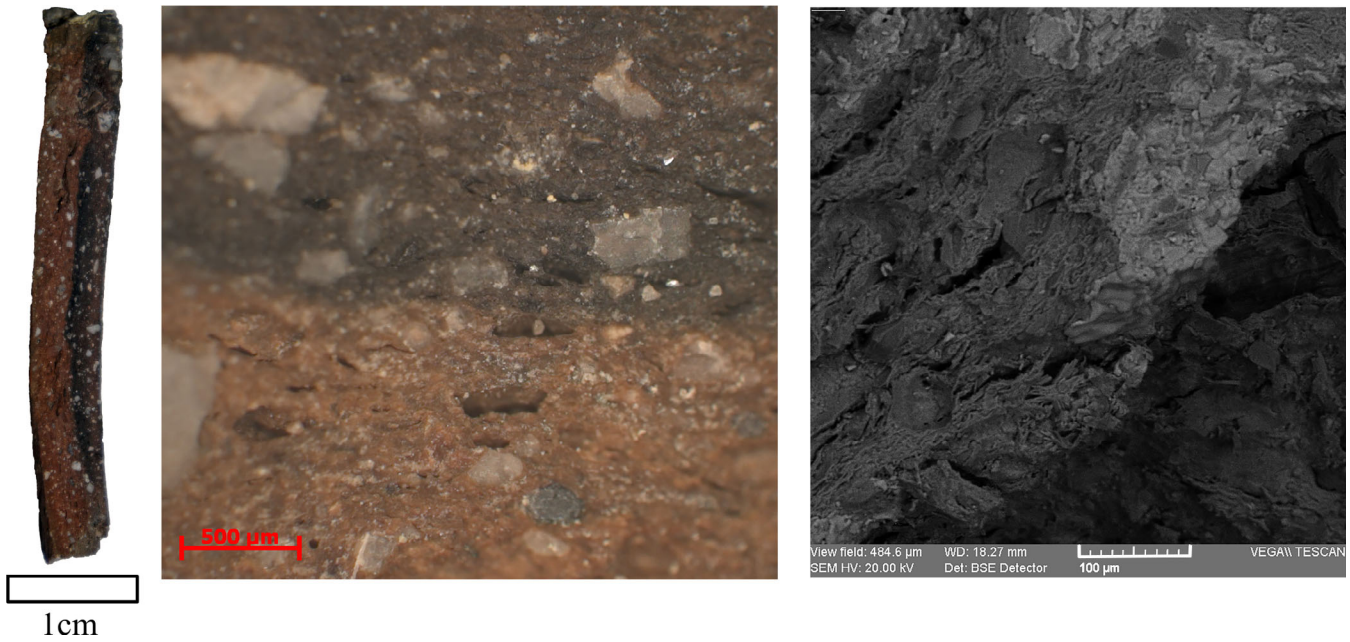


**FIGURE 9** Sample S15317: (a) macroscopic photograph, (b) OM and (c) SEM images. OM, optical microscopy; SEM, scanning electron microscopy with energy-dispersive X-ray spectrometry [Color figure can be viewed at wileyonlinelibrary.com]

contaminants from the soil during underground lying. Furthermore, several samples have small quantities of phosphorus (S14763, S15278, S15282, and S15321) under 0.4%, while others have sulfur (S14763, S15278, S15282, S15317, S16645, S16667, and S17713) in concentrations between 0.02% and 3.19%. Samples S14763, S15150, S15282, and S16667 contain carbon on only one of the analyzed areas, while S15157 has a concentration of 1.4377% in the core of the sample, meaning that the object from which it originates was fired at a temperature under 800°C.

Almost all the analyzed samples have Na and Cl, but the concentrations are low. For samples S14763, S15278, S153317, and S16642, the concentrations of Na vary from 4% to 10% and those of Cl from 3% to 11% and are found predominantly in the reddish area, corresponding to the oxidizing firing. In the case of sample S17713, the concentrations of Na and Cl are 20% and 19%, respectively, which occur in the case of reducing firing, this sample having even saline deposits macroscopically observable. The results show that the oxidizing atmosphere seems to be more

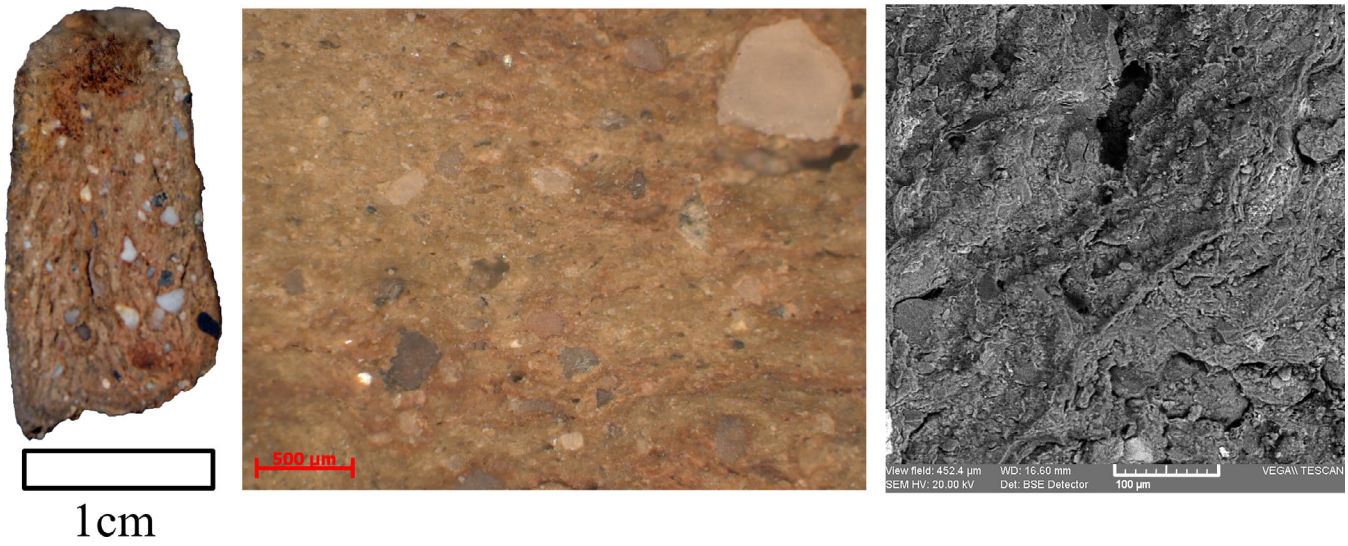


**FIGURE 10** Sample S15321: (a) macroscopic photograph, (b) OM and (c) SEM images. OM, optical microscopy; SEM, scanning electron microscopy with energy-dispersive X-ray spectrometry [Color figure can be viewed at wileyonlinelibrary.com]

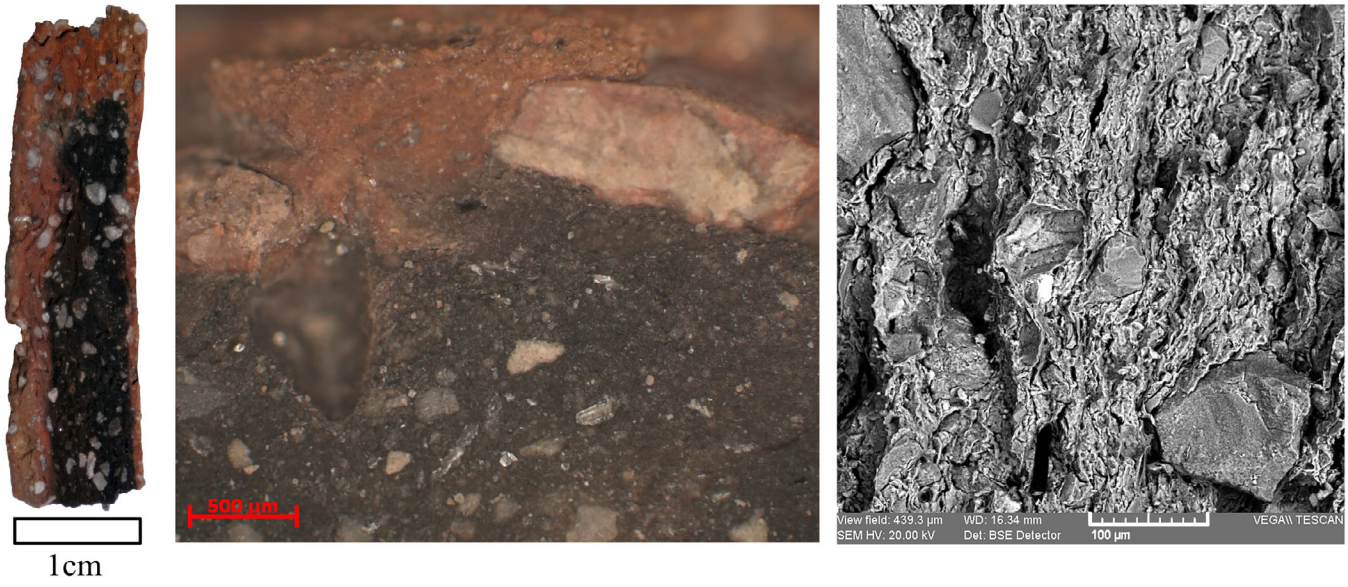


**FIGURE 11** Sample S16642: (a) macroscopic photograph, (b) OM and (c) SEM images. OM, optical microscopy; SEM, scanning electron microscopy with energy-dispersive X-ray spectrometry [Color figure can be viewed at wileyonlinelibrary.com]

related to the elements indicating the presence of salt than the reducing one.

The interpretation of these results can be done in two directions: the relatively low concentrations of salt can come from soil contamination, and the highest ones can be from during the use-life of the vessel. Considering the fact that one of the samples had a different medium (yellow, sterile soil) and does not show any trace of salt, it can support the first interpretation, namely, that of soil contamination, but only in the case of concentrations with small values.

The five ceramic fragments (S14763, S15278, S153317, S16642, and S17713) with high concentrations of Na and Cl may come from vessels that have been used for salt exploitation. Also, although the fragments are atypical, the decoration may indicate certain ceramic shapes, namely, jar pots or bowls. Jar pots are storage vessels that could be used for storage or transport of brine, and bowls could be used to evaporate this liquid. Thus, the analyses carried out may indicate a possible use of these vessels in the processing of the salt from the settlement at Băile Figa.

The high Fe content (above 4% on average) demonstrates that ferruginous clay was used for manufacturing the artifacts. The absence of carbon from the composition of some of the samples proves that the objects were fired at temperatures above 800°C. Calcite resists up to 800°C, above which it decomposes into CaO following the formation of the so-called "crystalline phase at high temperature" from calcium

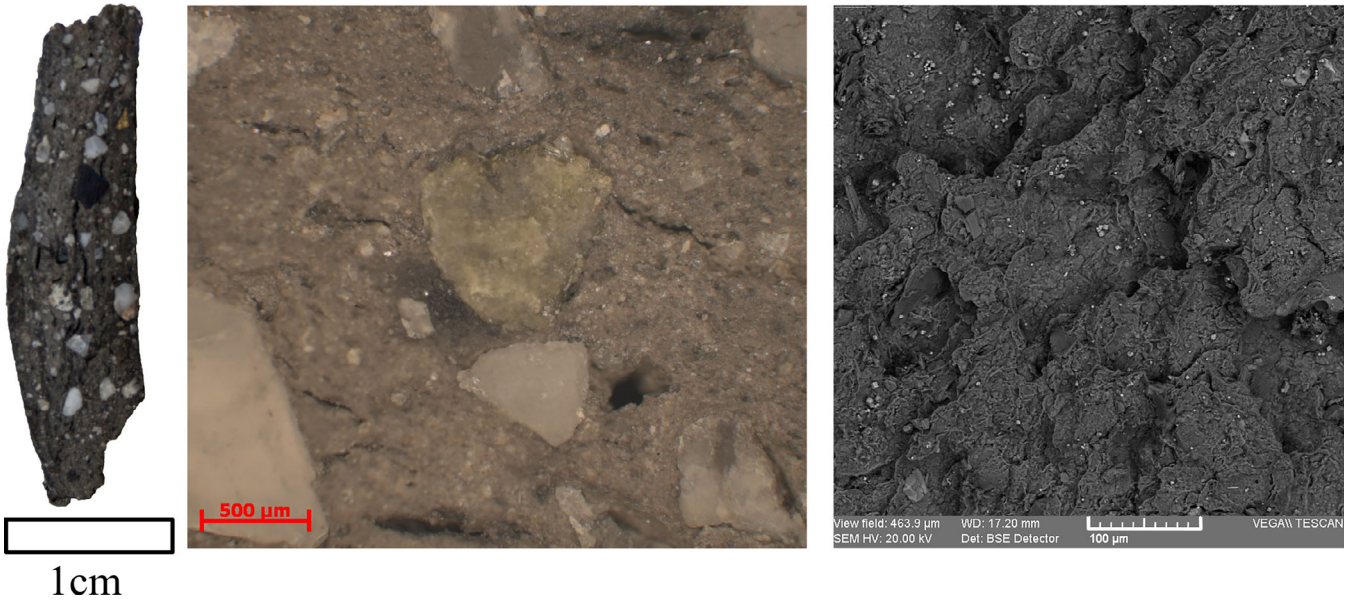


**FIGURE 12** Sample S16645: (a) macroscopic photograph, (b) OM and (c) SEM images. OM, optical microscopy; SEM, scanning electron microscopy with energy-dispersive X-ray spectrometry [Color figure can be viewed at wileyonlinelibrary.com]

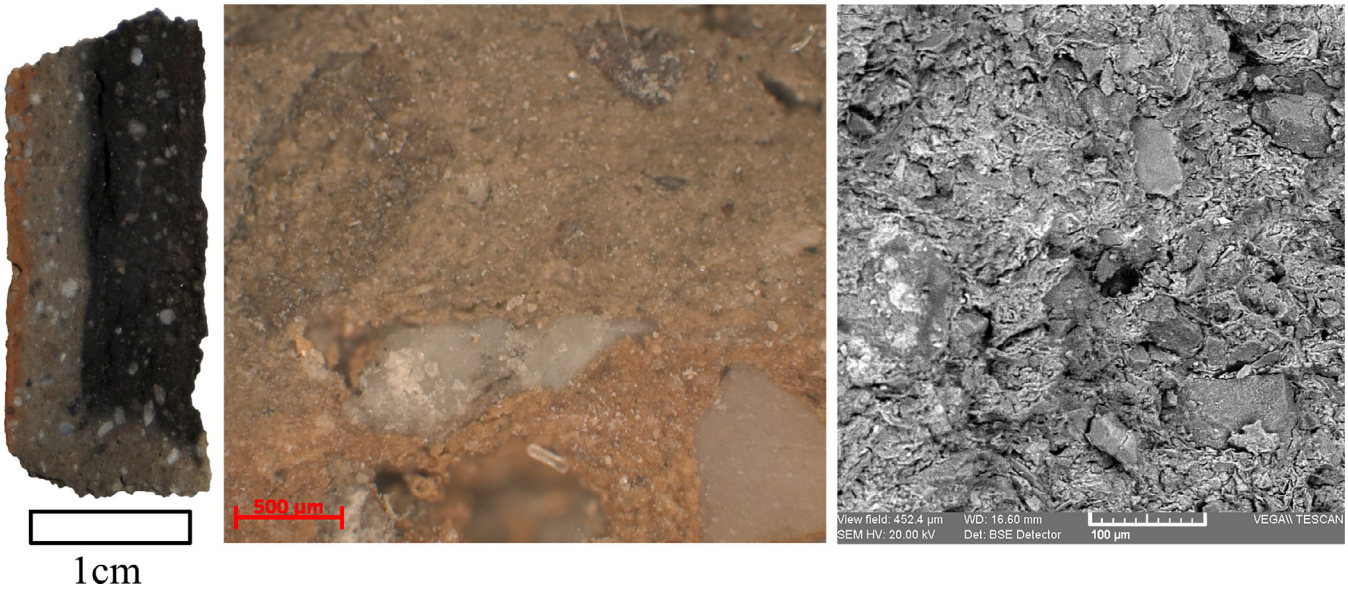


**FIGURE 13** Sample S16667: (a) macroscopic photograph, (b) OM and (c) SEM images. OM, optical microscopy; SEM, scanning electron microscopy with energy-dispersive X-ray spectrometry [Color figure can be viewed at wileyonlinelibrary.com]

silicates or Ca-Al silicates, such as gehlenite ($CaAl_2SiO_7$), diopside ($CaMgSi_2O_6$), and anorthite ($CaAl_2Si_2O_8$) (Nodari, Marcuz, Maritan, Mazzoli, & Russo, 2007; Nodari, Maritan, Mazzoli, & Russo, 2004; Ravisankar, 2009; Ravisankar, Chandrasekaran, Kiruba, Senthilkumar, & Maheswaran, 2010; Ravisankar, Kiruba, Eswaran, Senthilkumar, & Chandrasekaran, 2010; Ravisankar, Rajalakshimi, & Manicandan, 2006).

By comparing the elemental composition on the two surfaces analyzed on sample S14763, we find that Na, Cl, and Ca have greater values on the red area, which is to the outside, than on the black one. This is explained by the fact that the fragment was laid in a soil with a high content of salt. The other part may have sat on another potshard and was not in direct contact with the soil.

The objects from ceramics fired at temperatures under 950°C (nonvitrified) have high porosity, and through the variation of the humidity, the salts can react, leading to their breaking or decomposition. The ceramics fired at high temperature, which is vitrified, are impermeable to water and, accordingly, cannon be deteriorated by the soluble salts (Sandu, Cotiugă, et al., 2010; Sandu, Vasilache, et al., 2010).

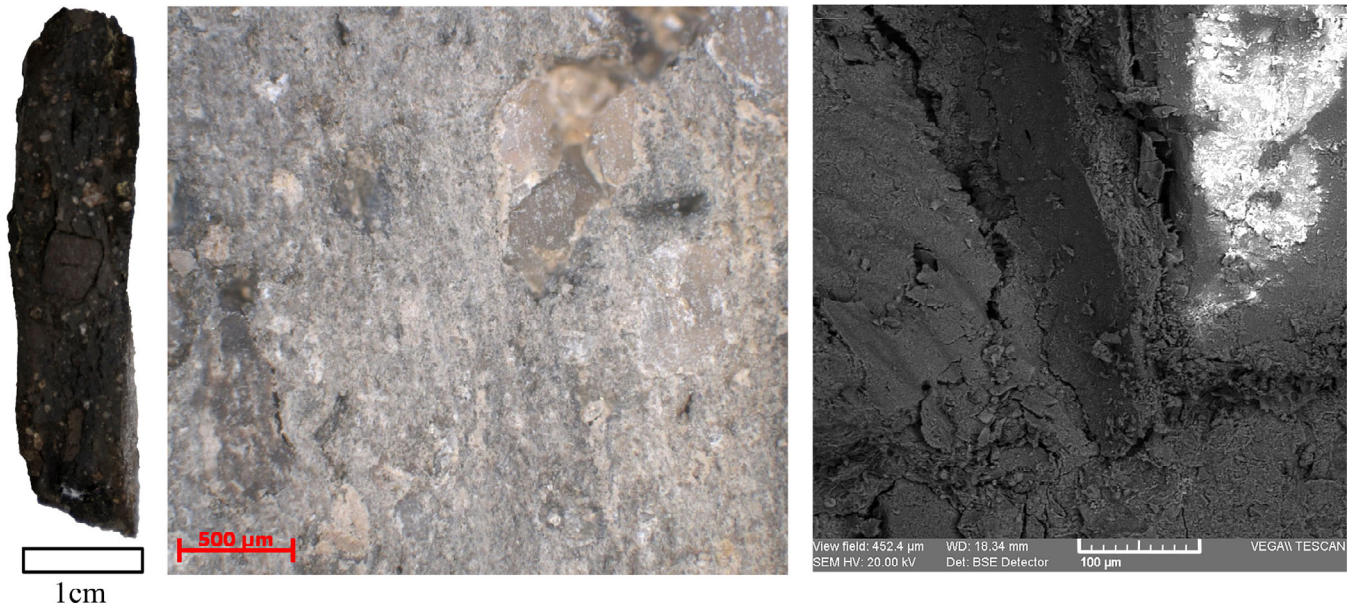


**FIGURE 14** Sample S17713: (a) macroscopic photograph, (b) OM and (c) SEM images. OM, optical microscopy; SEM, scanning electron microscopy with energy-dispersive X-ray spectrometry [Color figure can be viewed at wileyonlinelibrary.com]

**TABLE 1** The elemental composition of the ceramic samples

| | | Elemental composition—Weight percentages | | | | | | | | | | | | |
|---|---|---|---|---|---|---|---|---|---|---|---|---|---|---|
| Sample | | Si | Al | Fe | Ca | Mg | K | Na | Ti | Cl | P | S | C | O |
| S14763 | Red | 20.3284 | 8.1265 | 3.2766 | 4.1442 | 0.1305 | 1.4823 | 3.7095 | 0.9806 | 3.0453 | 0.0798 | 2.1532 | – | 52.5432 |
| | Black | 24.2289 | 10.4547 | 3.7388 | 0.5646 | 0.4969 | 1.2926 | 2.8117 | 0.8575 | 0.7249 | 0.3406 | – | 0.5613 | 53.9274 |
| S15150 | Red | 28.3495 | 9.8425 | 4.4548 | 0.6851 | 0.5705 | 1.9383 | 2.1838 | 1.0021 | 0.6790 | – | – | 0.6903 | 49.6039 |
| | Black | 29.4769 | 9.8024 | 4.1538 | 0.5067 | 0.6890 | 1.6484 | 2.2365 | 0.6358 | 0.6123 | – | – | – | 50.2379 |
| S15157 | | 25.8923 | 9.8393 | 5.0749 | 1.0061 | 0.7464 | 1.4328 | 1.2185 | 0.5195 | – | – | – | 1.4377 | 52.8324 |
| S15278 | Red | 20.6298 | 7.7367 | 3.7169 | 0.3419 | 0.1065 | 1.1915 | 8.0930 | 0.8263 | 8.6186 | 0.1845 | 0.0283 | – | 48.5259 |
| | Gray | 28.4419 | 10.3718 | 5.1667 | 0.5342 | 0.7913 | 1.2133 | 2.4270 | 0.6029 | 1.0793 | – | – | – | 49.3715 |
| | Black | 27.5801 | 10.0339 | 5.4825 | 0.7704 | 0.5319 | 1.6539 | 1.5951 | 0.8015 | 0.7597 | – | – | – | 50.7911 |
| S15282 | Red | 20.3502 | 8.3197 | 8.9169 | 0.6250 | 0.1508 | 1.0476 | 2.0896 | 0.8248 | 0.6112 | 0.3384 | 0.1559 | 1.9849 | 54.5849 |
| | Black | 22.4907 | 8.4734 | 4.9129 | 0.2986 | 0.1812 | 0.9183 | 2.2316 | 0.4611 | 0.3494 | 0.1103 | – | – | 59.5724 |
| S15317 | Red | 17.7637 | 6.6060 | 5.7569 | 0.5284 | 0.3059 | 1.4211 | 10.3656 | 0.6269 | 11.1364 | – | 0.9349 | – | 44.5542 |
| | Black | 15.2940 | 6.9652 | 4.7609 | 1.5440 | 0.3019 | 0.6727 | 8.4647 | 0.4656 | 5.2682 | – | 3.0972 | – | 53.1655 |
| S15321 | | 25.4244 | 9.3549 | 5.2379 | 0.1817 | 0.6723 | 1.1048 | 3.4458 | 0.6950 | 0.7609 | 0.1339 | – | – | 52.9883 |
| S16642 | Red | 21.2625 | 7.8601 | 4.0302 | 0.3511 | 0.6694 | 1.3909 | 10.2141 | 0.6015 | 8.6952 | – | – | – | 44.9252 |
| | Black | 28.6702 | 9.4726 | 3.5797 | 0.6779 | 0.9356 | 1.8484 | 3.2731 | 0.7380 | 0.9305 | – | – | – | 49.8738 |
| S16645 | Core | 22.0100 | 8.7722 | 5.9341 | 0.6597 | 0.9154 | 1.7703 | 2.2042 | 0.7481 | 0.7117 | – | 2.1427 | – | 54.1317 |
| S16667 | Red | 24.3111 | 9.2937 | 6.3924 | 0.8306 | 1.1025 | 2.5316 | 1.3869 | 0.8881 | 0.2525 | – | 0.9999 | – | 52.0108 |
| | Gray | 24.8504 | 8.7084 | 6.5099 | 0.5099 | 0.8236 | 2.2386 | 1.3489 | 0.6587 | 0.1589 | – | 0.6262 | – | 53.5665 |
| | Black | 23.7073 | 8.4974 | 5.2955 | 0.3848 | 0.6882 | 2.0341 | 1.4488 | 0.7313 | 0.6151 | – | - | 1.7392 | 54.8583 |
| S17713 | Black | 27.3886 | 3.8483 | 5.4902 | 0.8292 | 0.2515 | 1.0255 | 2.3127 | 0.9164 | 1.4987 | – | 3.1999 | – | 53.2388 |
| | Gray | 24.0115 | 9.0776 | 4.4011 | 0.9465 | 1.0587 | 2.2588 | 1.6439 | 0.5557 | 0.3093 | – | 0.6035 | – | 55.1334 |
| | Surfaces with salt | 5.3820 | 1.9012 | 3.0899 | 2.1999 | 0.0714 | 0.7545 | 19.7495 | – | 18.7239 | – | 4.6614 | – | 43.4663 |

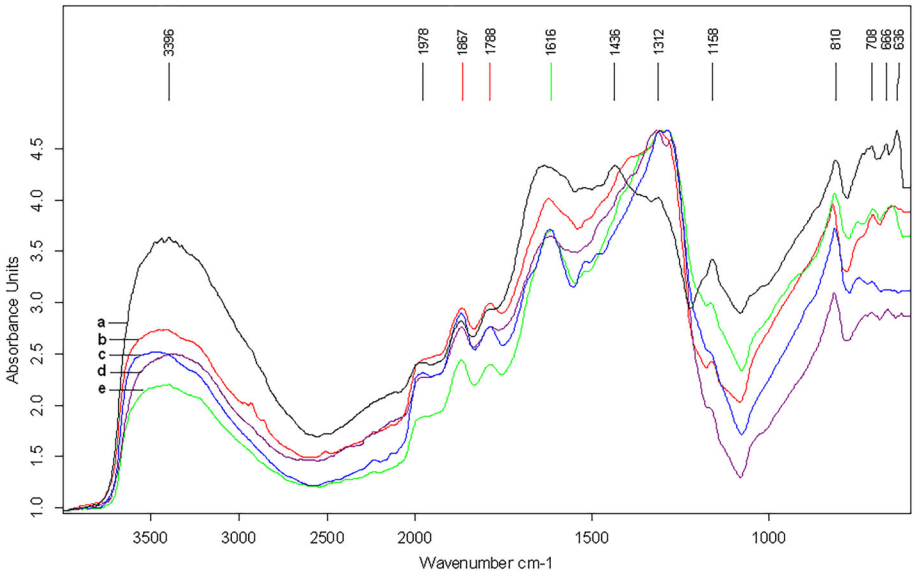


**FIGURE 15** The micro-FTIR spectra for the samples in which C were identified by the EDX analysis: (a) S15157, (b) S14763, (c) S15150, (d) S15282, and (e) S16667. EDX, energy-dispersive X-ray spectrometry; FTIR, Fourier-transform infrared spectroscopy [Color figure can be viewed at wileyonlinelibrary.com]

Because following the EDX analysis samples S14763, S15150, S15282, and S16667 revealed the presence of C on one of the analyzed areas, and in S15157 it is present across the entire material, the samples were analyzed by means of micro-FTIR in order to establish the nature of the compounds on the basis of the characteristic group vibrations.

Figure 15 presents five overlapping micro-FTIR spectra afferent to each analyzed sample, marked as follows: (a) S15157, (b) S14763, (c) S15150, (d) S15282, and, (e) S16667. The peak from 1436 $cm^{-1}$ corresponding to the carbonate band present only in the spectra demonstrates that the vessel from which this fragment originated was fired at a temperature below 800°C, while the rest were fired at temperatures above 800°C. The presence of C in the rest of the samples is due to contamination.

In all the samples, the wide band around 3396 $cm^{-1}$ and the medium one from 1616 $cm^{-1}$, which are attributed to the OH group from water were also identified. The peak at 1158 $cm^{-1}$ corresponds to silicates (Si-O) from quartz, while the peak from 666 $cm^{-1}$ corresponds to magnetite ($Fe_3O_4$), the peak from 636 $cm^{-1}$ is for feldspar (Fieldes, Furkert, & Wells, 1972; Shepherd, Kiefer, & Graham, 1986), and the peak from 810 $cm^{-1}$ is attributed to muscovite, which is stable up to 950°C. Its presence in all the samples indicates that the objects were burned to 950°C (Barilaro et al., 2008; Benedetto et al., 2002; Palanivel & Velraj, 2007; Russell, 1987; Shoval, Yadin, & Panczer, 2011; Velraj et al., 2009; Velraj et al., 2015).

## 4 | CONCLUSIONS

The pottery analyzed in this study belongs to the category of coarse ware, and it often has its exterior, and sometimes its interior, decorated with striations or brush lines.

Through analysis using the coassisted techniques OM, SEM–EDX, and micro-FTIR, we obtained a series of data concerning the morphology and chemical composition, on the basis of which the nature of the lithic material, the manufacturing technology, and the burning system were ascertained.

EDX analysis showed in all the ceramic samples the presence of the elements Si, Al, Fe, Ca, Mg Na, K, and O, meaning that they contain aluminosilicates, quartz, iron oxides (magnetite), and feldspar.

The case of the vessels with high concentrations of Na and Cl shows that they were used in the exploitation of salt. Conversely, those with low values of Na and Cl have these elements present from later contamination in the underground environment. The iron content, averaging 4%, shows that the raw material is of ferruginous nature. With the exception of S15157, all the fragments were fired at a temperature above 800°C in a predominantly reducing atmosphere.

## ACKNOWLEDGMENT

This work was supported by a grant of Ministry of Research and Innovation, CNCS—UEFISCDI, project number 151/2017, PN-III-P4-ID-PCE-2016-0759, within PNCDI III, *The Ethnoarchaeology of Salt in the Inner Carpathian area of Romania*—ethnosalro.uaic.ro.

## ORCID

*Viorica Vasilache* https://orcid.org/0000-0002-8866-3460

## REFERENCES

Barilaro, D., Barone, G., Crupia, V., Majolino, D., Mazzoleni, P., Tigano, G., & Venuti, V. (2008). FT-IR absorbance spectroscopy to study Sicilian "proto-majolica" pottery. *Vibrational Spectroscopy*, *48*(2), 269–275. https://doi.org/10.1016/j.vibspec.2008.01.005

Benedetto, G. E., Laviano, R., Sabbatini, L., & Zambonin, P. G. (2002). Infrared spectroscopy in the mineralogical characterization of ancient pottery. *Journal of Cultural Heritage*, *3*, 177–186.

Cavruc, V., Buzea, D. L., Puskás, J., Ştefan, M., Zăgreanu, R., Popa, I., & Semeniuc, A. I. (2015). Cercetări arheologice efectuate la Băile Figa în anul 2015. Secţiunea XV. Raport preliminar. *Angustia*, *19*, 55–112.

Cotiugă, V., Sandu, I., Vasilache, V., & Ursulescu, N. (2012). Atypical local accumulation of calcium carbonate deposits in prehistoric ceramics

during underground lying. In V. Cotiuga & S. Caliniuc (Eds.), *Interdisciplinarity research in archaeology* (pp. 209–214). Oxford: BAR International Archaeopress Series 2433.

Drebushchak, V. A., Mylnikova, L. N., Drebushchak, T. N., & Boldyrev, V. V. (2005). The investigations of ancient pottery. *Journal of Thermal Analysis and Calorimetry*, *82*(3), 617–626. https://doi.org/10.1007/s10973-005-0942-9

Fieldes, M., Furkert, R. J., & Wells, N. (1972). Rapid determination of constituents of whole soils using infrared absorption. *NZ Journal of Science*, *15*, 615–627.

Forster, N., Grave, P., Vickery, N., & Kealhofer, L. (2011). Non-destructive analysis using PXRF: Methodology and application to archaeological ceramics. *X-RAY Spectrometry*, *40*, 389–398. https://doi.org/10.1002/xrs.1360

Froh, J. (2004). Archeological ceramics studied by scanning electron microscopy. *Hyperfine Interactions*, *154*(1–4), 159–176.

Gaboyer, F., Le Milbeau, C., Bohmeier, M., Schwendner, P., Vannier, P., Beblo-Vranesevic, K., … Westall, F. (2017). Mineralization and preservation of an extremotolerant bacterium isolated from an early Mars analog environment. *Scientific Reports*, *7*, Article number: 8775, 14p. https://doi.org/10.1038/s41598-017-08929-4

Goodall, R. A., Hall, J., Viel, R., & Fredericks, P. M. (2007). A spectroscopic investigation of pigment and ceramic samples from Copan, Honduras. *Archaeometry*, *51*, 95–109. https://doi.org/10.1111/j.1475-4754.2007.00382.x

Hajjaji, M., Kacim, S., & Boulmane, M. (2002). Mineralogy and firing characteristics of a clay from the valley of Ourika. *Applied Clay Science*, *21*, 203–212.

Harding, A., & Kavruk, V. (2013). *Explorations in salt archaeology in the Carpathian Zone*. Budapest, Hungary: Archaeolingua.

Hunt, A. M. W., & Speakman, R. J. (2015). Portable XRF analysis of archaeological sediments and ceramics. *Journal of Archaeological Science*, *53*, 626–638. https://doi.org/10.1016/j.jas.2014.11.031

Ionescu, C., Ghergari, L., Horga, M., & Radulescu, G. (2007). Early medieval ceramics from the Viile Tecii archeological site (Romania): An optical and XRD study. *Studia Universitiatis Babes-Bolyai*, *Geologia*, *52*(2), 29–35. https://doi.org/10.5038/1937-8602.52.2.4

Iordanidis, A., Garcia, Guinea, J., & Karamitrou Mentessidi, G. (2009). Analytical study of ancient pottery from the archeological site of Aiani, Northern Greece. *Materials Characterization*, *60*(4), 292–302. https://doi.org/10.1016/j.matchar.2008.08.001

Kacsó, C., Metzner-Nebelsick, C., & Nebelsick, L. D. (2011). New work at the Late Bronze Age tumulus cemetery of Lăpuş in Romania. In *Ancestral landscapes. TMO 58* (pp. 341–353). Lyon: Maison de l'Orient et de la Méditerranée.

Krapukaityte, A., Tautkus, S., Kareiva, A., & Zelickiene, E. (2008). Thermal analysis—A powerful tool for the characterization of pottery. *Chemija*, *19*(2), 4–8.

Maggetti, M. (1994). Mineralogical and petrographical methods for the study of ancient pottery. In F. Burragato, O. Grubessi, & L. Lazzarini (Eds.), *First European workshop on archaeological ceramics* (pp. 23–35). Rome: Università La Sapienza.

Manoharan, C., Venkatachalapathy, R., Dhanapandian, S., & Deenadayalan, K. (2007). FTIR and Mossbauer spectroscopy applied to study of archeological artifacts from Maligaimedu, Tamilnadu, India. *Indian Journal of Pure and Applied Physics*, *45*(10), 860–865.

Merkevicius, A., Bezdicka, P., Juskenas, R., Kiuberis, J., Senvaitiene, J., Pakutinskiene, I., & Kareiva, A. (2007). XRD and SEM characterization of archeological findings excavated in Lithuania. *Chemija*, *18*(1), 36–39.

Mitchell, D., Grave, P., Maccheroni, M., & Gelman, E. (2012). Geochemical characterisation of north Asian glazed stonewares: A comparative analysis of NAA, ICP-OES and non-destructive pXRF. *Journal of Archaeological Science*, *39*(9), 2921–2933. https://doi.org/10.1016/j.jas.2012.04.044

Munsell Color. (2009). *Munsell soil-color charts*. Grand Rapids, MI: Munsell Color.

Naseerutheen, A., Ravisankar, R., Rajalakshmi, A., Raja Annamalai, G., & Chandrasekaran, A. (2013). FT-IR spectroscopic studies of ancient pottery from Kaveripakkam, Vellore Dist, Tamilnadu, India. *International Journal of Chemical Studies*, *1*(4), 45–49.

Nodari, L., Marcuz, E., Maritan, L., Mazzoli, C., & Russo, U. (2007). Hematite nucleation and growth in the firing of carbonate-rich clay for pottery production. *Journal of the European Ceramic Society*, *27*, 4665–4673. https://doi.org/10.1016/j.jeurceramsoc.2007.03.031

Nodari, L., Maritan, L., Mazzoli, C., & Russo, U. (2004). Sandwich structures in the Etruscan-Padan typepottery. *Applied Clay Science*, *27*, 119–128. https://doi.org/10.1016/j.clay.2004.03.003

Palanivel, R., & Rajesh Kumar, U. (2011). Thermal and spectroscopic analysis of ancient potteries. *Romanian Journal of Physics*, *56*(1–2), 195–208.

Palanivel, R., & Velraj, G. (2007). FTIR and FT-Raman spectroscopic studies of fired clay artifacts recently excavated in Tamilnadu, India. *Indian Journal of Pure and Applied Physics*, *45*, 501–508.

Papachristodoulou, C., Oikonomou, A., Ioannides, K., & Gravani, K. (2006). A study of ancient pottery by means of X-ray fluorescence spectroscopy, multivariate statistics and mineralogical analysis. *Analytica Chimica Acta*, *573*(SI), 347–353. https://doi.org/10.1016/j.aca.2006.02.012

Ravisankar, R. (2009). Application of spectroscopic techniques for the identification of minerals from beach rocks of Tamilnadu, India. *Exploration and Research for Atomic Minerals*, *19*, 272–276.

Ravisankar, R., Chandrasekaran, A., Kiruba, S., Senthilkumar, G., & Maheswaran, C. (2010). Analysis of ancient potteries of Tamilnadu, India by spectroscopic techniques. *Indian Journal of Science and Technology*, *3*(8), 858–862.

Ravisankar, R., Kiruba, S., Eswaran, P., Senthilkumar, G., & Chandrasekaran, A. (2010). Mineralogical characterization studies of ancient potteries of Tamilnadu, India by FT-IR spectroscopic technique. *E-Journal of Chemistry*, *7*(S1), S185–S190.

Ravisankar, R., Kiruba, S., Shamira, C., Naseerutheen, A., Balaji, P. D., & Seran, M. (2011). Spectroscopic techniques applied to the characterization of recently excavated ancient potteries from Thiruverkadu Tamilnadu, India. *Microchemical Journal*, *99*(2), 370–375. https://doi.org/10.1016/j.microc.2011.06.012

Ravisankar, R., Rajalakshimi, A., & Manicandan, E. (2006). Mineral characterization of soil samples in and around saltfield area Kelambakkam, Tamilnadu, India. *Acta Ciencia Indica*, *XXXII*(3), 341–346.

Rice, P. M. (1999). On the origins of pottery. *Journal of Archaeological Method and Theory*, *6*, 1–54.

Russell, J. D. (1987). Infrared methods. In M. J. Wilson (Ed.), *A handbook of determinative methods in clay mineralogy* (pp. 133–173). New York: Blackie & Son Ltd.

Sandu, I., Cotiugă, V., Sandu, A. V., Ciocan, A. C., Olteanu, G. I., & Vasilache, V. (2010). New archaeometric characteristics for ancient pottery identification. *International Journal of Conservation Science*, *1*(2), 75–82.

Sandu, I., Vasilache, V., Tencariu, F.A., Cotiugă, V. (2010). *Conservarea Ştiinţifică a Artefactelor din Ceramică*, Iaşi, Ed. Universităţii "Al.I. Cuza".

Shepherd, R. A., Kiefer, W. S., & Graham, W. R. M. (1986). Characterization of the Circle Cliffs Tar Sands: 1. Application of the FTIR technique to mineral matter. *Fuel*, *65*, 1261–1264.

Shoval, S. (2003). Using FTIR spectroscopy for study of calcareous ancient ceramics. *Optical Materials*, *24*(1, 2-SI), 117–122. https://doi.org/10.1016/S0925-3467(03)00114-9

Shoval, S., Yadin, E., & Panczer, G. (2011). Analysis of thermal phases in calcareous iron age pottery using FT-IR and Raman spectroscopy. *Journal of Thermal Analysis and Calorimetry*, *104*, 515–525. https://doi.org/10.1007/s10973-011-1518-5

Tite, M. S. (1999). Pottery production, distribution, and consumption: The contribution of the physical sciences. *Journal of Archaeological Method and Theory*, *6*(3), 181–233.

Tsolakidou, A., Buxeda, i., Garrigós, J., & Kilikoglou, V. (2002). Assessment of dissolution techniques for the analysis of ceramic samples by plasma spectrometry. *Analytica Chimica Acta*, *474*(1–2), 177–188. https://doi.org/10.1016/S0003-2670(02)01029-2

Tsolakidou, A., & Kilikoglou, V. (2002). Comparative analysis of ancient ceramics by neutron activation analysis, inductively coupled plasma–optical-emission spectrometry, inductively coupled plasma–mass spectrometry, and X-ray fluorescence. *Analytical and Bioanalytical Chemistry*, *374*(3), 566–572. https://doi.org/10.1007/s00216-002-1444-2

Velraj, G., Janaki, K., Mohamed Musthafa, A., & Palnivel, R. (2009). Estimation of firing temperature of some archeological pottery shreds excavated recently in Tamilnadu, India. *Spectrachemica Acta, Part A: Molecular and Bimolecular Spectroscopy*, *72*(4), 730–733. https://doi.org/10.1016/j.saa.2008.11.015

Velraj, G., Tamilarasu, S., & Ramya, R. (2015). FTIR, XRD and SEM-EDS studies of archaeological pottery samples from recently excavated site in Tamil Nadu, India. *Materials Today: Proceedings*, *2*, 934–942. https://doi.org/10.1016/j.matpr.2015.06.012

**How to cite this article:** Vasilache V, Kavruk V, Tencariu F-A. OM, SEM–EDX, and micro-FTIR analysis of the Bronze Age pottery from the Băile Figa salt production site (Transylvania, Romania). *Microsc Res Tech*. 2020;1–14. https://doi.org/10.1002/jemt.23451